A BTB/POZ protein, NAC-1, is related to tumor recurrence and is essential for tumor growth and survival

Kentaro Nakayama*, Naomi Nakayama*, Ben Davidson†, Jim J.-C. Sheu*, Natini Jinawath*, Antonio Santillan‡§, Ritu Salani‡§, Robert E. Bristow‡§, Patrice J. Morin¶, Robert J. Kurman*‡§, Tian-Li Wang‡§, and Ie-Ming Shih*‡§‖

Departments of *Pathology, ‡Oncology, and §Gynecology and Obstetrics, Johns Hopkins Medical Institutions, Baltimore, MD 21231; †Norwegian Radium Hospital, 0310 Oslo, Norway; and ¶Laboratory of Cellular and Molecular Biology, National Institute on Aging, National Institutes of Health, Baltimore, MD 21224

Edited by Joan S. Brugge, Harvard Medical School, Boston, MA, and approved October 8, 2006 (received for review May 18, 2006)

Recent studies have suggested an oncogenic role of the BTB/POZ-domain genes in hematopoietic malignancy. The aim of this study is to identify and characterize BTB/POZ-domain genes in the development of human epithelial cancers, i.e., carcinomas. In this study, we focused on ovarian carcinoma and analyzed gene expression levels using the serial analysis of gene expression (SAGE) data in all 130 deduced BTB/POZ genes. Our analysis reveals that NAC-1 is significantly overexpressed in ovarian serous carcinomas and several other types of carcinomas. Immunohistochemistry studies in ovarian serous carcinomas demonstrate that NAC-1 is localized in discrete nuclear bodies (tentatively named NAC-1 bodies), and the levels of NAC-1 expression correlate with tumor recurrence. Furthermore, intense NAC-1 immunoreactivity in primary tumors predicts early recurrence in ovarian cancer. Both coimmunoprecipitation and double immunofluorescence staining demonstrate that NAC-1 molecules homooligomerize through the BTB/POZ domain. Induced expression of the NAC-1 mutant containing only the BTB/POZ domain disrupts NAC-1 bodies, prevents tumor formation, and promotes tumor cell apoptosis in established tumors in a mouse xenograft model. Overexpression of full-length NAC-1 enhanced tumorigenicity of ovarian surface epithelial cells and NIH 3T3 cells in athymic *nu/nu* mice. In summary, NAC-1 is a tumor recurrence-associated gene with oncogenic potential, and the interaction between BTB/POZ domains of NAC-1 proteins is critical to form the discrete NAC-1 nuclear bodies and essential for tumor cell proliferation and survival.

oncogene | ovarian cancer | serial analysis of gene expression

The BTB (bric-a-brac tramtrack broad complex) (also known as POZ) gene family is composed of several proteins that share a conserved BTB/POZ protein–protein interaction motif at the N terminus that mediates homodimer or heterodimer formation (1–3). These proteins have been demonstrated to participate in a wide variety of cellular functions including transcription regulation, cellular proliferation, apoptosis, cell morphology, ion channel assembly, and protein degradation through ubiquitination (1). A subset of BTB/POZ proteins have been implicated in human cancer, and they include BCL-6 (4, 5), PLZF (promyelocytic leukemia zinc finger) (4, 6), leukemia/lymphoma-related factor (LRF)/Pokemon (7, 8), HIC-1 (hypermethylated in cancer-1), and Kaiso (9, 10). Among them, the *BCL-6* gene is the best characterized oncogene. Frequent gene translocation or mutation has been identified in B cell lymphoma, resulting in constitutive BCL-6 expression in the tumor cells (4, 5). Peptide inhibitors that block interaction between the BCL-6 BTB/POZ domain and corepressors abrogate BCL-6 oncogenic functions in B cells, suggesting that the use of peptide inhibitors of the BTB/POZ domain may represent a therapeutic approach for B cell lymphoma (5). As the role of BTB/POZ proteins in human cancer is emerging, we have analyzed the expression patterns of tumor-associated BTB/POZ genes in ovarian cancer *in silico* using the serial analysis of gene expression (SAGE) database. Ovarian cancer was selected in this study because this disease represents one of the most aggressive cancer types in women. Most patients with ovarian cancer are diagnosed at advanced stages when conventional therapy is less effective. As a result, most ovarian cancer patients suffer from, and eventually succumb to, recurrent disease. New therapeutic agents are urgently needed for effective treatment to improve outcome in these patients. In this study, we focused on a BTB/POZ gene, *NAC-1*, that is overexpressed in ovarian cancer, particularly in recurrent disease. We demonstrated that *NAC-1* plays a critical role in tumorigenesis and in the growth and survival of tumor cells.

Results

NAC-1 Expression Is Associated with Cancer Development. A total of 11 SAGE libraries were used to screen 130 BTB/POZ domain-containing genes for overexpression in high-grade ovarian serous carcinomas as compared with ovarian surface epithelium and benign ovarian cystadenoma. Sixteen genes were selected based on an average tag count per library >10 (Table 2, which is published as supporting information on the PNAS web site). Among these 16 genes, a gene named *NAC-1* (BTBD14B HS.531614) showed the highest ratio of average tag counts in ovarian carcinoma to controls (ovarian surface epithelium and benign ovarian cyst) and was therefore selected for validation and characterization in this study. The SAGE database was also used to analyze *NAC-1* expression in different cancer types and their corresponding normal tissues. As shown in Fig. 1, in addition to ovarian cancer, NAC-1 was upregulated in several tumors from other organs including pancreatic, colorectal, and breast carcinomas, although the sample size of SAGE libraries in most of tumor types was too small for a statistical analysis.

To validate the SAGE results in ovarian cancer, we generated a mouse monoclonal antibody (NAC-1 Ab clone 3) that reacted to the C terminus of the NAC-1 protein and performed immunohistochemistry in 265 ovarian tumors and normal tissue samples (Table 3, which is published as supporting information on the PNAS web site). The specificity of the NAC-1 antibody was evaluated by

MEDICAL SCIENCES

Author contributions: K.N., N.N., T.-L.W., and I.-M.S. designed research; K.N., N.J., and N.N. performed research; B.D., J.J.-C.S., R.E.B., P.J.M., and R.J.K. contributed new reagents/analytic tools; K.N., N.N., A.S., R.S., T.-L.W., and I.-M.S. analyzed data; and K.N., T.-L.W. and I.-M.S. wrote the paper.

The authors declare no conflict of interest.

This article is a PNAS direct submission.

Abbreviations: JHMI, Johns Hopkins Medical Institutions; MOSE, immortalized OSE cells; NRH, Norwegian National Radium Hospital; OSE, ovarian surface epithelial cells; SAGE, serial analysis of gene expression.

Data deposition: The sequence reported in this paper has been deposited in the UniGene database, www.ncbi.nlm.nih.gov/entrez/guery.fcgi?db-unigene (accession no. HS.531614).

‖To whom correspondence should be addressed at: Johns Hopkins Hospital, CRB II, Room 305, 1550 Orleans Street, Baltimore, MD 21231. E-mail: ishih@jhmi.edu.

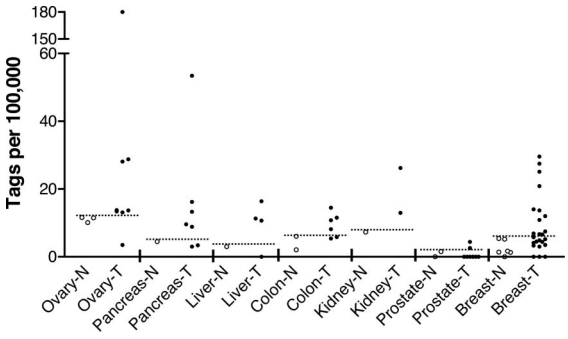

Fig. 1. Scatter plot of NAC-1 tags in several major tumor types. NAC-1 expression level is analyzed by counting NAC-1-specific tags from SAGE libraries in both cancer tissue (T, filled symbols) and the corresponding normal tissues (N, open symbols). The NAC-1 tags are normalized to tags per 100,000 (*y* axis). The dash line in each tumor type indicates the ''ceiling'' tag number in normal tissue libraries. Each symbol represents an individual specimen.

reciprocal immunoprecipitation/Western blot analyses in RK3E cells transfected with pCDNA6-V5/NAC-1 and vector control. A single band with a molecular mass of ≈57 kDa corresponding to NAC-1 protein was detected in *NAC-1*-transfected cells but not in control cells (Fig. 2*A*). Because the immunoreactive tumor cells always exhibited diffuse staining, we used intensity scores to quantify NAC-1 expression in tissues. In contrast to normal ovaries and benign ovarian cystadenomas, both low- and high-grade serous carcinomas demonstrated a higher NAC-1 immunoreactivity, with 27% and 40% of cases showing 2+ and 3+, respectively (χ^2 test, $P < 0.001$) (Fig. 2 *B–D* and Table 3). The number of high-grade cases with high NAC-1 immunointensity (2+ and 3+) was significantly higher than that in low-grade carcinoma ($P < 0.01$). Immunofluorescence revealed that NAC-1 was localized to dot-like structures in those tumors showing strong NAC-1 immunointensity (2+ and 3+) (Fig. 2 *E* and *F*). Ultrastructural analysis using ImmunoGold labeling, and electron microscopy further revealed that NAC-1 was localized to discrete nuclear bodies, tentatively termed "NAC-1 bodies", with a diameter ranging from 0.3 to 1.8 μm (Fig. 2*G*).

Overexpression of NAC-1 Correlates with Recurrent Ovarian Cancer. It is widely accepted that recurrent tumors represent the true "killer" in cancer patients, because the primary tumors are usually removed by surgery. Identification of molecular targets that are present in recurrent tumors would be important in the development of a prognostic test and a novel therapeutic intervention for cancer patients. Thus, we addressed whether NAC-1 expression was related to tumor progression by analyzing primary and recurrent ovarian high-grade serous carcinomas using immunohistochemistry and quantitative real-time PCR. NAC-1 immunohistochemistry was performed at two institutions, Johns Hopkins Medical Institutions (JHMI, solid tumors) and Norwegian National Radium Hospital (NRH, effusions), by using independent sets of ovarian cancer specimens, and the results are presented in a 2 × 2 contingency table (Table 1). Among 182 JHMI high-grade carcinoma cases, we analyzed 166 samples including 110 primary and 56 first recurrent tumors. The remaining 16 specimens that were obtained from second and third recurrence were not included in the analysis. Both JHMI and NRH studies demonstrated that a higher NAC-1 staining intensity (2+ and 3+) was more frequently found in recurrent than in primary tumor tissues ($P < 0.01$ in JHMI and $P = 0.013$ in NRH, χ^2 test). To validate the immunohistochemistry results, we performed quantitative real-time PCR using samples from JHMI to assess the correlation of *NAC-1* mRNA expression levels and the recurrence status. We found that an increased *NAC-1* transcript level significantly correlated with recurrent disease ($P = 0.012$, Mann–Whitney test) (Fig. 3*A*). The association of NAC-1 expression and recurrent status was independent of clinical stage (III versus IV) at diagnosis.

Among 56 recurrent carcinomas from JHMI, there were 21 cases for which the corresponding primary tumors were available from the same patients for comparison. A statistically significant increase in NAC-1 immunointensity (2+ and 3+) was found in recurrent tumors as compared with the primary tumors from the same

Table 1. Increased NAC-1 immunoreactivity correlates with first tumor recurrence

	JHMI (solid tumors)		NRH (effusions)	
	0+/1+	2+/3+	0+/1+	2+/3+
Primary	71	39	62	49
First recurrent	21	35	22	39
Total	92	74	84	88

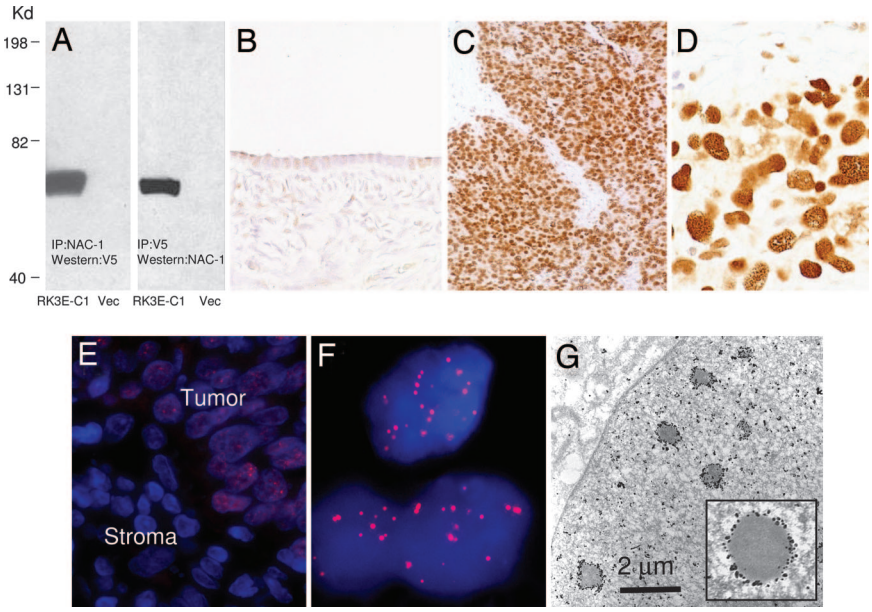

Fig. 2. Immunoreactivity of NAC-1 in ovarian cancer tissues. (*A*) Immunoprecipitation/Western blot analyses using NAC-1 and V5 antibodies in RK3E cells transfected with pCDNA6-NAC-1/V5 (RK3E-C1) or vector-only control (Vec). A discrete band corresponding to NAC-1 protein mass is identified in this reciprocal analysis. (*B–D*) The NAC-1 immunointensity is undetectable or weak in normal ovarian surface epithelium (*B*) but is strong in a high-grade serous carcinoma (*C* and *D*). (*E* and *F*) Immunofluorescence of NAC-1 protein localization in ovarian cancer cells in a tissue section. Tumor cells contain NAC-1 protein, which is located in discrete nuclear bodies (*E*). The adjacent stromal cells are negative for NAC-1 immunoreactivity. A higher magnification demonstrates the NAC-1 nuclear bodies by using a confocal fluorescence microscope (*F*). (*G*) Ultrastructure of NAC-1 bodies. ImmunoGold labeling of NAC-1-expressing RK3E cells demonstrates electron-dense bodies decorated by gold particles in the nuclear matrix.

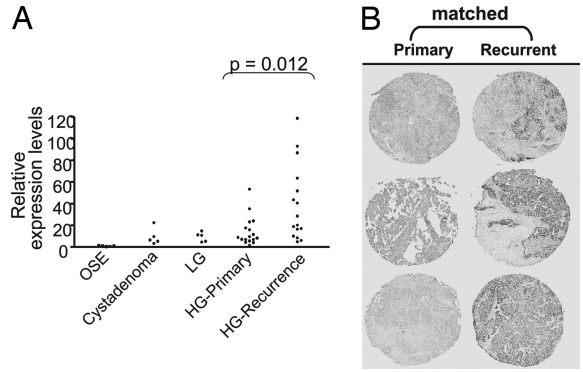

Fig. 3. NAC1 expression correlates with tumor progression in ovarian serous carcinomas. (*A*) Quantitative real-time PCR analysis shows higher NAC-1 expression levels in high-grade carcinomas (HG) than in ovarian surface epithelial cells (OSE), low-grade carcinomas (LG), and cystadenomas. Moreover, recurrent carcinomas have significantly higher expression levels than primary tumors ($P = 0.012$). The data are expressed as fold increase as compared with the average of OSE. (*B*) Immunohistochemistry demonstrates intense immunoreactivity in recurrent tumors as compared with patients' primary tumors in three representative cases.

patients ($P = 0.017$, χ^2 test) (Fig. 3*B*). Based on these findings, we further analyzed to see whether *NAC-1* expression in primary tumors was predicative of disease-free interval (the period between primary surgery and tumor recurrence) in 57 patients with advanced-stage high-grade serous carcinomas who underwent optimal primary debulking surgery, followed by a standard chemotherapeutic regimen in the same institution (JHMI). We found that high NAC-1 immunointensity (2+ and 3+) predicted recurrence within 1 year after diagnosis with an odds ratio of 14.9 (95% CI, 3.00–74.2; $P = 0.0002$, Fisher's exact test). The median disease-free interval with NAC-1 immunointensity of ≥2 was 12 months, whereas when the intensity was <2, the interval was 18 months.

The positive correlation of NAC-1 expression and recurrent disease suggests that NAC-1 plays a role in the development of recurrent ovarian tumors. To test whether NAC-1 expression directly contributes to drug resistance, we correlated NAC-1 immunoreactivity and *in vitro* drug resistance in 60 high-grade serous carcinomas. The *in vitro* drug-resistance results were performed at Oncotech (Tustin, CA) by using the protocol described at www.oncotech.com/pdfs/edr_4_pager.pdf (11, 12). Cases were grouped according to different immunointensity scores, but there was no significant correlation ($P > 0.17$, χ^2 test) between NAC-1 expression and *in vitro* resistance to carboplatin, cisplatin, and taxol, the standard chemotherapeutic agents for ovarian cancer.

Dominant Negative Role of NAC-1 BTB/POZ Domain. Because the BTB/POZ domain has been known to be involved in protein homomerization or heteromerization, we tested whether the NAC-1 BTB/POZ domain participated in protein–protein interaction using deletion mutants of NAC-1 (Fig. 4*A*). Based on coimmunoprecipitation and immunofluorescence colocalization studies (Fig. 4 *B* and *C*), we found that the BTB/POZ domain of NAC-1, corresponding to the 1–129 aa at the N terminus (N130 construct), was the minimal structural motif required for NAC-1 homooligomerization (Fig. 4*B*). The *NAC-1* deletion mutants/Xpress tags were then transfected into RK3E cells that had been stably transfected with a full-length NAC-1/V5 tag expression vector. As shown in Fig. 4*C*, full-length NAC-1/V5 colocalized with the full-length NAC-1/Xpress in the NAC-1 bodies, indicating that NAC-1 interacted with NAC-1. As expected, both *N130* and *N250* deletion mutants containing the BTB/POZ domain also colocalized with full-length *NAC-1*, but interestingly, both mutants disrupted the formation of NAC-1 bodies by transforming them into "cotton candy"-like aggregates or large "noodle"-like structures in the nuclei (Fig. 4*C*). In contrast, *C250* and *M120* deletion mutants that did not contain the BTB/POZ domain failed to colocalize with wild-type NAC-1.

Suppression of Tumor Formation upon Induction of NAC-1 N130 Mutant. To test whether the BTB/POZ domain is involved in tumor growth, we established an inducible (Tet-Off) system by expressing the N130 construct upon removal of doxycycline in two *NAC-1*-positive tumor cell lines, SKOV3, an ovarian cancer cell line, and HeLa, a cervical adenocarcinoma cell line. Cervical adenocarcinomas, like ovarian serous carcinomas, frequently overexpressed NAC-1, because a high level of NAC-1 immunoreactivity (2+ and 3+) occurred in ≈50% (16 of 32) cervical adenocarcinomas, whereas the NAC-1 immunoreactivity in normal endocervical glands were undetectable (Fig. 7, which is published as supporting information on the PNAS web site).

For both SKOV3-N130 and HeLa-N130 cell lines, the efficiency of N130 induction was very high as evidenced by >99% of cells expressing green fluorescence based on flow cytometry (data not shown) and increased copy number of N-terminal mRNA sequence as compared with C-terminal sequence based on quantitative real-time PCR (Fig. 8 *A* and *B*, which is published as supporting information on the PNAS web site) after removal of doxycycline. Like RK3E cells expressing the *N130* mutant (Fig. 4*C*), NAC-1 nuclear bodies were transformed to cotton candy-like aggregates in

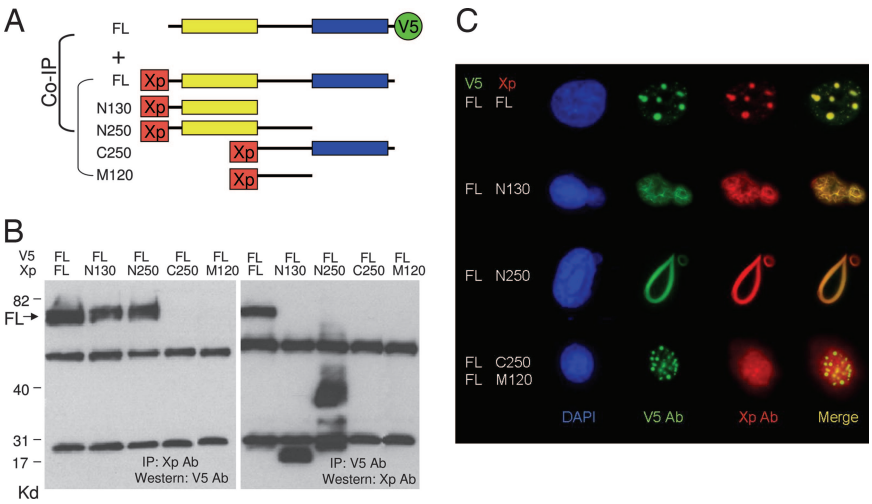

Fig. 4. Coimmunoprecipitation and colocalization of NAC-1 deletion mutants and full-length NAC-1. (*A*) Diagram of NAC-1 and NAC-1 deletion mutants. Full-length (FL) construct contains V5 tag at the C terminus, whereas all of the deletion mutants contain an Xpress (Xp) tag at the N terminus. The yellow box is the BTB/POZ domain; the blue box is the DUF1172 domain. (*B*) Coimmunoprecipitation shows that full-length NAC-1, N130, and N250 bind to NAC-1. The predicted molecular masses, not including the tag sequences, are: full-length NAC-1 (57.3 kDa), N130 (14.4 kDa), N250 (27.8 kDa), C250 (30.3 kDa), and M120 (14 kDa). (*C*) Cells with stable full-length NAC-1/V5 expression were transfected with different deletion mutants with the Xp tag. Double immunofluorescence shows that full-length NAC-1, N130, and N250 deletion mutants colocalize with full-length NAC-1. However, only full-length NAC-1 proteins form discrete round and oval-shaped NAC-1 nuclear bodies ,whereas both N130 and N250 form irregular aggregates with the full-length NAC-1. Neither C250 nor M120 colocalizes with the full-length NAC-1 protein.

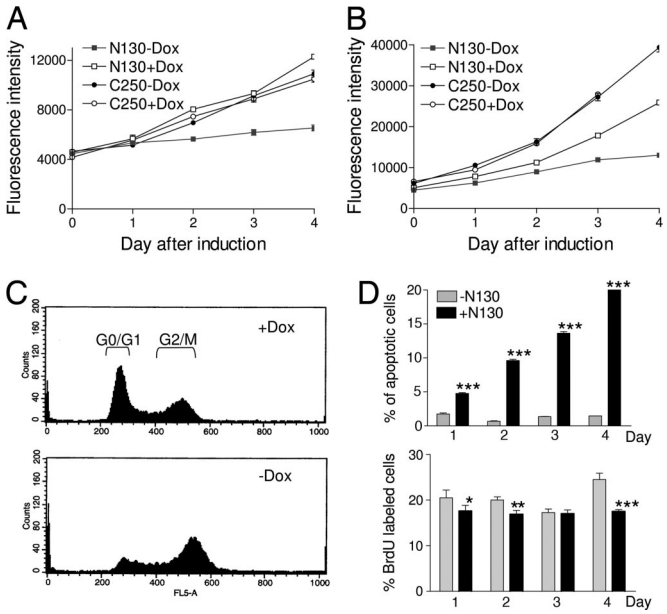

Fig. 5. Effects of N130 induction on cellular proliferation and apoptosis in 96-well plates. (*A* and *B*) Cell growth curves show that after induction of N130 (−Dox), cell growth is significantly suppressed as compared with the noninduced cells (+Dox). In contrast, induction of C250 does not have an apparent effect on cell growth in SKOV3 (*A*) or HeLa (*B*) cells. (*C*) Cell cycle analysis shows an increase in G_2/M fraction in N130-induced HeLa cells (*Lower*) as compared with noninduced cells (*Upper*) 24 h after induction, indicating a G_2/M block. (*D*) Percentages of apoptotic and proliferating cells are determined by counting annexin V- and BrdU-positive cells, respectively, in both N130-induced and -noninduced cells. Data are presented as mean + SD. *, $P < 0.05$; **, $P < 0.001$, ***, $P < 0.0001$, Student's *t* test.

both SKOV3 and HeLa cells after induction of *N130* (Fig. 8*C*). As compared with the control (induction of C250), induction of *N130* expression significantly reduced cell proliferation in both SKOV3 cells (Fig. 5*A*) and HeLa cells (Fig. 5*B*). Induction of the control *C250* mutant did not have significant effects on cellular proliferation in either of the cell lines. Similarly, expression of *N130* significantly suppressed colony formation in both cell lines (Fig. 9, which is published as supporting information on the PNAS web site). The decrease in cellular growth after *N130* induction was associated with cell cycle arrest at G_2/M phase (percentage of cells in G_0/G_1-to-S-to-G_2/M = 50.3%-to-16.5%-to33.2% in noninduced cells vs. 20.1%-to-17.4%-to-62.5% in induced cells) (Fig. 5*C*). *N130* induction significantly increased the number of annexin V-labeled cells and also decreased the number of BrdU-labeled cells (except on day 3), although the level in the decrease of cells with BrdU uptake is not as dramatic as the increase of annexin V-labeled cells (Fig. 5*D*). To further evaluate the effect of N130 on cellular proliferation and apoptosis, we used the miniN130 mutants, N65 and N30-122, in which its BTB/POZ oligomerization activity was deficient. Both N65 and N30-122 showed protein expression but were not able to coimmunoprecipitate with the full-length NAC-1 protein (Fig. 10*A*, which is published as supporting information on the PNAS web site). When transfecting these two constructs into the NAC-1 overexpressing SKOV3 cells, both N65 and N30-122 could not effectively suppress cellular proliferation as compared with N130 (Fig. 10*B*). In addition, we also knocked down NAC-1 using RNAi to determine whether there was a similar inhibitory effect to the expression of the N130 dominant-negative construct. In fact, NAC-1-expressing SKOV3 and HeLa cells had significantly reduced cell numbers after NAC-1 siRNA treatment (Fig. 11 *A* and *B*, which is published as supporting information on the PNAS web site). In contrast, NAC-1 siRNA did not show a significant effect on the cell growth of OVCAR3 cells that did not express abundant NAC-1 (Fig. 11*B*). Furthermore, we found that the apoptosis-inducing effect of the siRNAs used here was potent, but was less pronounced than the N130 dominant-negative NAC-1 (Fig. 11*C*), indicating that the latter approach could be a more effective experimental system to inactivate NAC-1 function. As a control, we expressed N130 in OVCAR3, which expressed only a minimal amount of NAC-1 protein compared with HeLa and SKOV3 cells, and found that N130 expression did not have a significant effect on the growth of OVCAR3 cells (Fig. 11*D*).

Based on the above findings, we investigated whether disrupting interactions between NAC-1 molecules using the N130 dominant-negative approach had a growth-inhibitory effect in HeLa (Fig. 12, which is published as supporting information on the PNAS web site) and SKOV3 (Fig. 13, which is published as supporting information on the PNAS web site) xenografts in nude mice. First, we tested whether expression of N130 could prevent tumorigenesis by inducing N130 expression 2 days after s.c. tumor injection. As shown in Figs. 12*A* and 13*A*, induction of N130 expression in HeLa and SKOV3 cells almost completely prevented the formation of s.c. tumors. In contrast, the control cells grew tumors at all injection sites. Second, we determined whether N130 could limit tumor growth in established HeLa and SKOV3 tumors. The expression of N130 was induced by removing doxycycline, when all of the mice harbor palpable tumors. Five days after discontinuation of doxycycline, induction of N130 expression was evidenced by green fluorescence in the s.c. HeLa tumors because expression of both N130 and EGFP was driven by a bicistronic promoter (Fig. 12*B*). As shown in Figs. 12*C* and 13*B*, tumors continued growing in control mice, whereas the tumors stopped growing or decreased in size after N130 induction. Histological examination of the tumors excised 10 days after N130 induction revealed extensive apoptosis in tumor cells, based on morphology and immunoreactivity with the M30 antibody, which recognizes the apoptosis-specific caspase-cleaved cytokeratin epitope (13, 14) (Fig. 12*D*).

The Oncogenic Potential of NAC-1 Expression. To test whether NAC-1 expression is tumorigenic, we randomly selected two clones from a spontaneously immortalized MOSE cell line and two NIH 3T3 clones that were stably transfected with an NAC-1 expression vector (Fig. 6). When compared with vector-transfected controls, all NAC-1-expressing clones had a higher cellular proliferation, based on growth curves and BrdU-uptake assays (Fig. 6 *A*, *D*, and *F*). S.c. injections of NAC-1-expressing MOSE clones in athymic *nu*/*nu* mice produced larger tumors than the control cells transfected with the vector-only (Fig. 6 *B* and *C*). MOSE clones did not grow i.p. tumors 21 days after i.p. injection. The NAC-1-expressing NIH 3T3 clones produce both s.c. and i.p. tumors in the athymic *nu*/*nu* mice. The i.p. tumors were always multiple, and their combined weights were measured in each mouse (Fig. 6*E*). In contrast, the vector-transfected NIH 3T3 cells did not grow tumors during the course of this study.

Discussion

NAC-1 was first identified and cloned as a transcript induced in the nucleus accumbens from rats treated with cocaine (15). The nucleus accumbens is a unique forebrain structure involved in reward motivation (16) and many addictive behaviors (17–19). Except for its role in cocaine-induced expression in animal brains, the cellular function of NAC-1 is unknown. In this study, we demonstrate that *NAC-1* is a previously uncharacterized cancer-associated gene, because the NAC-1 expression level is significantly increased in several types of cancers including ovarian cancer, cervical adenocarcinoma, and breast cancer. We showed that NAC-1 was required for cell proliferation and survival and was sufficient to enhance tumorigenicity in athymic *nu*/*nu* mice.

Cancer mortality and morbidity are related to recurrent and metastatic disease. Therefore, a positive correlation between

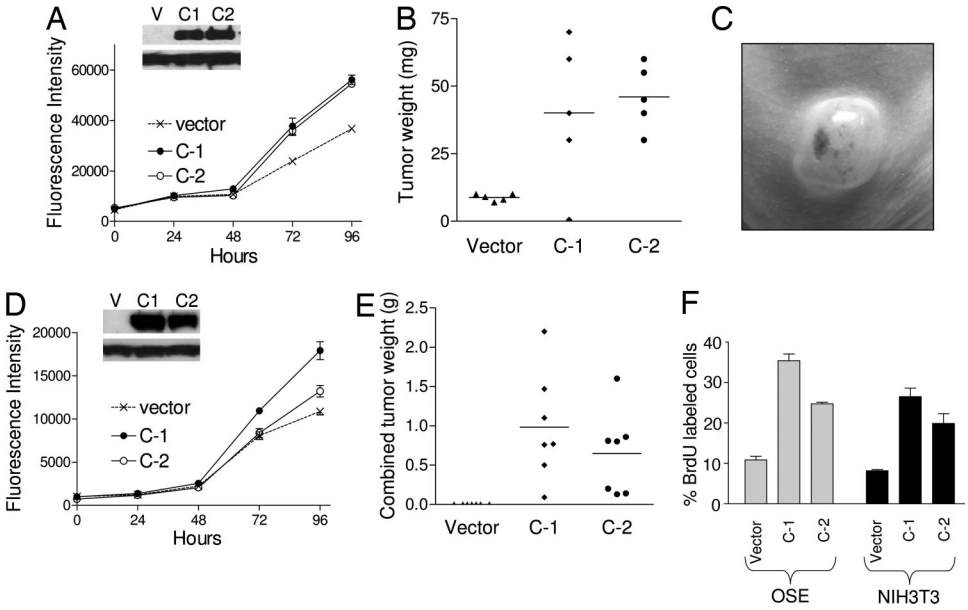

Fig. 6. Effects of constitutive expression of NAC-1 in immortalized ovarian surface epithelial cells (MOSE) and NIH 3T3 cells. Western blot analysis shows NAC-1 expression in stable clones of NAC-1-expressing MOSE cells (*A*) and NIH 3T3 cells (*D*). Upper blots, NAC-1; lower blots, GAPDH. Growth curves show a higher proliferation activity in both NAC-1 clones as compared with vector-transfected control under a low serum (0.5%) culture condition in MOSE cells (*A*) and NIH 3T3 cells (*D*). The weights of s.c. tumors increase in NAC-1-expressing MOSE tumors as compared with control MOSE in nude mice (*B*). A representative photomicrograph shows a s.c. NAC-1-expressing MOSE tumor (*C*). Similarly, the combined tumor weights of tumors in the peritoneal wall of the NAC-1-expressing NIH 3T3 cells are greater than the controls (*E*). (*F*) Cell proliferation was determined by a BrdU-incorporation assay, and all NAC-1-expressing clones have a higher proliferation rate than the vector-only control. Data are presented as mean + SD.

NAC-1 expression and recurrence status in ovarian carcinoma as shown in this study has significant biological and clinical implications. First, NAC-1 expression may directly contribute to tumor recurrence and tumor progression. However, a lack of correlation between NAC-1 expression and *in vitro* drug resistance to taxol, carboplatin, and cisplatin, the primary chemotherapeutic agents used in the treatment of ovarian cancer patients, suggests that NAC-1 may not directly participate in the development of drug resistance. Because the etiology of tumor recurrence is multifactorial, it is likely that NAC-1 overexpression confers a growth advantage to tumor cells by providing them with higher proliferative and lower apoptotic activity as shown in this study. Second, we demonstrated that intense NAC-1 immunoreactivity in primary tumors is highly predictive of a shorter disease-free interval; therefore, NAC-1 expression may potentially be used alone or in combination with other markers as a prognostic test to identify ovarian cancer patients who are likely to develop early recurrence. This finding can have potential clinical implications because at least 60% of advanced-stage ovarian cancer patients who appear to be disease-free after completing primary therapy ultimately develop recurrent disease (20). Thus, patients with NAC-1-positive ovarian serous carcinoma can be monitored more closely to detect recurrent tumor. It has been demonstrated that ovarian carcinoma patients can most benefit from secondary cytoreduction when the recurrent tumor is small and localized (20–24).

Similar to other BTB/POZ members, the NAC-1 BTB/POZ domain is essential and sufficient for NAC-1 homomerization. Based on immunoprecipitation using the NAC-1 antibody and tumor lysates from ovarian cancer tissues that expressed NAC-1, we did not detect other proteins that were pulled down with NAC-1, suggesting that NAC-1 molecules may homooligomerize to each other. The dominant-negative strategy using the *N130* deletion mutant suggests that homooligomerization of NAC-1 is required for formation of NAC-1 nuclear bodies. Although both *N130* and *N250* deletion mutants can be coimmunoprecipitated and colocalized with wild-type (full-length) NAC-1 molecules, they transformed the morphology of NAC-1 bodies, suggesting that both the BTB/POZ domain and the C-terminal motif of the NAC-1 molecule are critical for NAC-1 body formation. This finding is consistent with what has been observed in LAZ3/BCL6 proteins in which the BCL6 BTB/POZ domain has the capability to self-interact and target the protein to form discrete nuclear substructures (25). Furthermore, expression of the *N130* mutant but not miniN130 mutants that failed to bind to NAC-1 suppressed cellular proliferation and induced apoptosis, suggesting that interaction among NAC-1 molecules or between NAC-1 and other partner protein(s) through their BTB/POZ domains is essential for NAC-1-regulated tumor cell growth and survival. This result is similar to BCL-6 in which the peptide inhibitors that block interaction between the BCL-6 BTB/POZ domain and corepressors abrogate BCL-6 oncogenic functions in B cells and suggests that targeting the BTB/POZ domain of a specific BTB/POZ member may provide an approach for cancer therapy (5). Besides its critical role in maintaining cell proliferation and survival, NAC-1 expression could also enhance cellular proliferation and induce tumorigenicity in athymic *nu/nu* mice. These findings suggest that *NAC-1* is a gene with oncogenic potential in ovarian carcinomas.

In conclusion, this study shows that expression of NAC-1, a member of BTB/POZ family, is associated with the development of recurrent ovarian serous carcinoma. Homo-oligomerization of NAC-1 proteins through the BTB/POZ domains is essential for cell survival in carcinomas that express NAC-1. Targeting the BTB/POZ domain of NAC-1 could be a molecular strategy for drug intervention in ovarian cancer and other types of cancer with NAC-1 overexpression.

Materials and Methods

For detailed procedures of quantitative PCR, siRNA knockdown, and tumor xenograft assay, please see *Supporting Material and Methods*, which is published as supporting information on the PNAS web site.

Tag Counts of the BTB/POZ Family Genes from SAGE Libraries. Proteins matching the PS50097 profile of the BTB/POZ domain amino acid

sequence were extracted from the Swiss-Prot/TrEMBL protein databank released on January 16, 2006 (http://us.expasy.org/cgi-bin/get-entries?DR=PS50097&db=tr&db=sp&view=tree). A total of 130 BTB/POZ genes were identified. The expression levels of the BTB/POZ gene family members were determined from the ovarian tumor SAGE libraries by obtaining the SAGE tag counts for each BTB/POZ gene. The libraries included the OSE cells (SV-40 immortalized IOSE29 (26) and short-term cultured HOSE4), benign cystadenoma (ML10), ovarian high-grade serous carcinoma tissues (HG63, HG48, HG92, OVT6, OVT7, and OVT8), and ovarian cancer cell lines (OVCAR3 and A2780). All libraries have been published (27), except HG63, HG48 and HG92 which were established in this study. The NAC-1-specific SAGE tags included TTCCCGGCCC, TGAAGGCAGT, CCTATAATCG, AGTGCCAGGG, AGAATATCAG, GAGGGAGGGA, and GTTCCCCCAC. By using a minimum tag count setting of >1, these NAC-1 tags were tallied and normalized per 100,000 total tags for each SAGE library. To select the candidate gene(s) for further study, we first select those with a high average tag count (>10 tags per 100,000 tags) in ovarian carcinoma libraries, followed by the highest ratio of average tag counts in ovarian carcinoma to the benign controls (IOSE29, HOSE4, and ML10).

To determine the NAC-1 expression levels among different cancer libraries, we compared NAC-1 tag counts among 81 SAGE libraries (http://cgap.nci.nih.gov/SAGE) (28, 29) from carcinomas and normal tissues of ovary, pancreas, liver, colon, kidney, prostate, and breast (30). NAC-1 tag counts for each library were retrieved by filtering for tag sequences that matched uniquely to NAC-1 according to the April 15, 2005 SAGEMap available on the public National Center for Biotechnology Information FTP site (ftp://ftp.ncbi.nlm.nih.gov/pub/sage/map/Hs/NlaIII).

Immunohistochemistry and Immunoelectron Microscopy. Paraffin-embedded tumor tissues were obtained from the Department of Pathology at the Johns Hopkins Hospital and effusion ovarian cancer samples were obtained from the Norwegian Radium National Hospital in Norway. These included 182 high-grade ovarian serous carcinoma tissues (154 stage III and 28 stage IV), 44 low-grade ovarian serous carcinoma tissues (42 stage III and 2 stage IV), 172 high-grade ovarian carcinoma effusion samples (1 stage I, 6 stage II, 97 stage III, and 68 stage IV), and 32 cervical adenocarcinomas. In addition, 21 benign ovarian cystadenomas, 18 normal ovaries, and 8 normal cervical tissues were included for comparison. Acquisition of tissue specimens and clinical information was approved by an institutional review board (Johns Hopkins Medical Institutions) or by the Regional Ethics Committee (Norwegian Radium Hospital).

For immunohistochemistry studies, we generated a mouse NAC-1 monoclonal antibody by immunizing mice with the NAC-1 recombinant protein using a standard hybridoma protocol (31). Immunohistochemistry was performed on deparaffinized sections by using the NAC-1 antibody at a dilution of 1:100 and an EnVision+System peroxidase kit (DAKO, Carpinteria, CA). Immunoreactivity was scored by two investigators as follows: 0, undetectable; 1+, weakly positive; 2+, moderately positive; and 3+, intensely positive. NAC-1 immunoreactivity was not detectable (immunointensity score = 0) or weak (1+) in normal OSE and benign serous cystadenomas. For ultrastructure study of NAC-1 bodies, we applied ImmunoGold labeling on NAC-1-expressing-RK3E cells, followed by electron microscopy.

Coimmunoprecipitation and Double Immunofluorescence Staining. A series of *NAC-1*-deletion mutants including N130 (encoding the amino acids 1–129 at the N terminus), N250 (amino acids 1–263 at the N terminus), M120 (amino acids 123–263 in the middle portion), and C250 (amino acids 257–528 at the C terminus) were generated by PCR. Both N130 and N250 mutants contained the BTB/POZ domain (amino acids 20–122) of NAC-1. In addition, two miniN130 expression constructs were generated, and they included N65 (encoding the first 1–65 aa of the BTB domain) and N30-122 (30–122 aa). PCR products of the *NAC-1*-deletion mutants were cloned into an expression vector, pCDNA4 with an Xpress tag at the N terminus. RK3E cells were first stably transfected with pCDNA6/V5/NAC-1 and then transiently transfected with the pCDNA4/NAC-1-deletion mutants. Coimmunoprecipitation was performed to assess the specific structural motifs that bound to full-length NAC-1. For immunofluorescence staining, cells were incubated with primary antibodies, followed by fluorescence-labeled secondary antibodies.

N130-Inducible Construct, Cell Proliferation, and Apoptosis Assays. The Tet-Off inducible system was used to assess the biological effects of N130. HeLa and SKOV3 cells that constitutively expressed tTA (tetracycline-controlled transactivator) were transfected with pBI-N130/EGFP or pBI-C250/V5-EGFP (control) that bicistronically expressed the products of interest and reporter EGFP upon the binding of tTA to the tetracycline-responsive element in the absence of inducer (doxycycline). Cell proliferation and apoptosis assays were performed as described (32) in 96-well plates.

We thank Mr. David Chu and Mr. M. Jim Yen for editorial assistance and Dr. C.-Y. Hsu for organization of cervical adenocarcinoma tissue microarrays. This study was supported by Department of Defense Grant OC0400600 and National Institutes of Health Grant CA103937.

1. Stogios PJ, Downs GS, Jauhal JJ, Nandra SK, Prive GG (2005) *Genome Biol* 6:R82.1–R82.17.
2. Bardwell VJ, Treisman R (1994) *Genes Dev* 8:1664–1677.
3. Albagli O, Dhordain P, Deweindt C, Lecocq G, Leprince D (1995) *Cell Growth Differ* 6:1193–1198.
4. Chen Z, Brand NJ, Chen A, Chen SJ, Tong JH, Wang ZY, Waxman S, Zelent A (1993) *EMBO J* 12:1161–1167.
5. Polo JM, Dell'Oso T, Ranuncolo SM, Cerchietti L, Beck D, Da Silva GF, Prive GG, Licht JD, Melnick A (2004) *Nat Med* 10:1329–1335.
6. Yeyati PL, Shaknovich R, Boterashvili S, Li J, Ball HJ, Waxman S, Nason-Burchenal K, Dmitrovsky E, Zelent A, Licht JD (1999) *Oncogene* 18:925–934.
7. Maeda T, Hobbs RM, Merghoub T, Guernah I, Zelent A, Cordon-Cardo C, Teruya-Feldstein J, Pandolfi PP (2005) *Nature* 433:278–285.
8. Maeda T, Hobbs RM, Pandolfi PP (2005) *Cancer Res* 65:8575–8578.
9. van Roy FM, McCrea PD (2005) *Nat Rev Cancer* 5:956–964.
10. Park JI, Kim SW, Lyons JP, Ji H, Nguyen TT, Cho K, Barton MC, Deroo T, Vleminckx K, Moon RT, McCrea PD (2005) *Dev Cell* 8:843–854.
11. Fruehauf JP, Alberts DS (2003) *Recent Results Cancer Res* 161:126–145.
12. Eltabbakh GH, Piver MS, Hempling RE, Recio FO, Lele SB, Marchetti DL, Baker TR, Blumenson LE (1998) *Gynecol Oncol* 70:392–397.
13. Leers M, Kolgen W, Bjorklund V, Bergman T, Tribbick G, Persson B, Bjorklund P, Ramaekers FC, Bjorklund B, Schutte B (1999) *J Pathol* 5:567–572.
14. Caulin C, Salvesen GS, Oshima RG (1997) *J Cell Biol* 138:1379–1394.
15. Cha XY, Pierce RC, Kalivas PW, Mackler SA (1997) *J Neurosci* 17:6864–6871.
16. Roitman MF, Wheeler RA, Carelli RM (2005) *Neuron* 45:587–597.
17. Koob GF (1996) *Neuron* 16:893–896.
18. Mackler SA, Korutla L, Cha XY, Koebbe MJ, Fournier KM, Bowers MS, Kalivas PW (2000) *J Neurosci* 20:6210–6217.
19. Kalivas PW, Duffy P, Mackler SA (1999) *Synapse* 33:153–159.
20. Diaz-Montes TP, Bristow RE (2005) *Curr Oncol Rep* 7:451–458.
21. Harter P, du Bois A (2005) *Curr Opin Oncol* 17:505–514.
22. Gadducci A, Iacconi P, Cosio S, Fanucchi A, Cristofani R, Riccardo Genazzani A (2000) *Gynecol Oncol* 79:344–349.
23. Gadducci A, Iacconi P, Fanucchi A, Cosio S, Teti G, Genazzani AR (2000) *Anticancer Res* 20:1959–1964.
24. Zang RY, Li ZT, Tang J, Cheng X, Cai SM, Zhang ZY, Teng NN (2004) *Cancer* 100:1152–1161.
25. Dhordain P, Albagli O, Ansieau S, Koken MH, Deweindt C, Quief S, Lantoine D, Leutz A, Kerckaert JP, Leprince D (1995) *Oncogene* 11:2689–2697.
26. Auersperg N, Pan J, Grove BD, Peterson T, Fisher J, Maines-Bandiera S, Somasiri A, Roskelley CD (1999) *Proc Natl Acad Sci USA* 96:6249–6254.
27. Hough CD, Sherman-Baust CA, Pizer ES, Montz FJ, Im DD, Rosenshein NB, Cho KR, Riggins GJ, Morin PJ (2000) *Cancer Res* 60:6281–6287.
28. Boon K, Osorio EC, Greenhut SF, Schaefer CF, Shoemaker J, Polyak K, Morin PJ, Buetow KH, Strausberg RL, De Souza SJ, Riggins GJ (2002) *Proc Natl Acad Sci USA* 99:11287–11292.
29. Lal A, Lash AE, Altschul SF, Velculescu V, Zhang L, McLendon RE, Marra MA, Prange C, Morin PJ, Polyak K, *et al.* (1999) *Cancer Res* 59:5403–5407.
30. Yen M-J, Hsu CY, Mao TT, Wu TC, Roden R, Wang TL, Shih IM (2006) *Clin Cancer Res* 12:827–831.
31. Shih IM, Elder DE, Speicher D, Johnson JP, Herlyn M (1994) *Cancer Res* 54:2514–2520.
32. Shih IM, Sheu JJ, Santillan A, Nakayama K, Yen MJ, Bristow RE, Vang R, Parmigiani G, Kurman RJ, Trope CG, *et al.* (2005) *Proc Natl Acad Sci USA* 102:14004–14009.